Article

Computational Study of Ketosteroid Isomerase: Insights from Molecular Dynamics Simulation of Enzyme Bound Substrate and Intermediate

Devleena Mazumder, Kalju Kahn, and Thomas C. Bruice

J. Am. Chem. Soc., **2003**, 125 (25), 7553-7561• DOI: 10.1021/ja030138s • Publication Date (Web): 30 May 2003

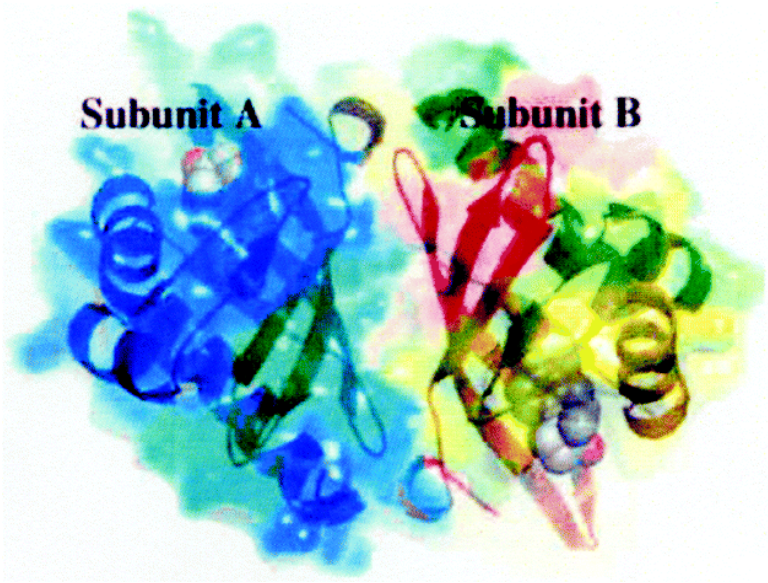

J|A|C|S
ARTICLES
Published on Web 05/30/2003

Computational Study of Ketosteroid Isomerase: Insights from Molecular Dynamics Simulation of Enzyme Bound Substrate and Intermediate

Devleena Mazumder, Kalju Kahn, and Thomas C. Bruice*

Contribution from the Department of Chemistry and Biochemistry, University of California, Santa Barbara, Santa Barbara, California 93106

Received February 26, 2003; E-mail: tcbruice@bioorganic.ucsb.edu.

Abstract: Δ^5-3-Ketosteroid Isomerase (KSI) catalyzes the isomerization of 5,6-unsaturated ketosteroids to their 4,5-unsaturated isomers at a rate approaching the diffusion limit. The isomerization reaction follows a two-step general acid−base mechanism starting with Asp38-CO_2^- mediated proton abstraction from a sp^3-hybridized carbon atom, α to carbonyl group, providing a dienolate intermediate. In the second step, Asp38-CO_2H protonates the C6 of the intermediate providing a 4,5-unsaturated ketosteroid. The details of the mechanism have been highly controversial despite several experimental and computational studies of this enzyme. The general acid−base catalysis has been proposed to involve either a catalytic diad or a cooperative hydrogen bond mechanism. In this paper, we report our results from the 1.5 nanosecond molecular dynamics (MD) simulation of enzyme bound natural substrate (E·S) and enzyme bound intermediate (E·In) solvated in a TIP3P water box. The final coordinates from our MD simulation strongly support the cooperative hydrogen bond mechanism. The MD simulation of E·S and E·In shows that both Tyr14 and Asp99 are hydrogen bonded to the O3 of the substrate or intermediate. The average hydrogen bonding distance between Tyr14-OH and O3 becomes shorter and exhibits less fluctuation on E·S → E·In. We also observe dynamic motions of water moving in and out of the active site in the E·S structures. This free movement of water disappears in the E·In structures. The active site is shielded by hydrophobic residues, which come together and squeeze out the waters from the active site in the E·In complex.

Introduction

Δ^5-3-Ketosteroid isomerase (KSI, EC 5.3.3.1) plays a crucial biological role of steroid transformation in animal tissues and microbial systems. KSI efficiently catalyzes proton abstraction from the C−H function adjacent (α) to carbonyl or carboxyl group.[1] Several well studied enzymes such as triosephosphate isomerase, citrate synthase, and Rubisco catalyze similar proton abstractions. A wide range of concepts including electrostatic stabilization, binding entropy, desolvation, orbital steering, participation of metal ions and short, strong low-barrier hydrogen bonds (LBHB) have been proposed to account for the rate acceleration of such reactions.[2−5]

KSI catalyzes the allylic isomerization of the 3-oxo-Δ^5-steroids, such as androst-5-ene-3,17-dione, to their conjugated Δ^4-isomers at a rate approaching the diffusion limit with k_{cat}/K_m of 3.0×10^8 M^{-1} s^{-1} (Scheme 1). The isomerization reaction has been proposed to follow a two-step general acid−base mechanism via a dienolate intermediate. The first step (Scheme 2) of the reaction involves general base (Asp38-CO_2^-) catalyzed abstraction of the β-proton from the C4 carbon atom of the steroid substrate (S) forming a dienolate intermediate (In), with

Scheme 1

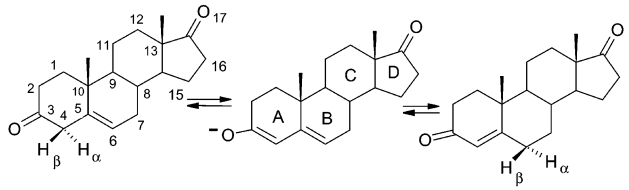

Substrate (S) Androst-5-ene-3,17-dione

Intermediate (In) 3-Hydroxy-androsta-3,5-dien-17-one

Tyr14 forming a hydrogen bond to the carbonyl oxygen O3 of substrate. The second step is a stereospecific proton transfer to the β-position at the allylic carbon C6 of intermediate by general acid Asp38-CO_2H.[1,6,7] The pK_{app} of Asp38 (in KSI from *Pseudomonas testosteroni*) is 4.57 in the free enzyme and 4.75 in the Michaelis complex.[8] Comparing the active sites of KSI from two different species, *Pseudomonas testosteroni* (TI) and *Pseudomonas putida* (PI), shows that Asp38 is surrounded by hydrophobic residues and has only one polar interaction with Trp120 in PI KSI whereas TI KSI enzyme lacks this polar interaction too. Therefore, it is important to answer the question of how does KSI maintain the pK_{app} of Asp38 to 4.75 in the

(1) Kuliopulos, A.; Talalay, P.; Mildvan, A. S. *Biochemistry* **1990**, *29*, 10 271.
(2) Warshel, A. *J. Biol. Chem.* **1998**, *273*, 27 035.
(3) Cleland, W. W.; Frey, P. A.; Gerlt, J. A. *J. Biol. Chem.* **1998**, *273*, 25 529.
(4) Cannon, W. R.; Benkovic, S. J. *J. Biol. Chem.* **1998**, *273*, 26 257.
(5) Cleland, W. W.; Kreevoy, M. M. *Science* **1994**, *264*, 1887.
(6) Bounds, P. L.; Pollack, R. M. *Biochemistry* **1987**, *26*, 2263.
(7) Zhao, Q.; Mildvan, A. S.; Talalay, P. *Biochemistry* **1995**, *34*, 426.
(8) Pollack, R. M.; Bantia, S.; Bounds, P. L.; Koffman, B. M. *Biochemistry* **1986**, *25*, 1905.

Scheme 2

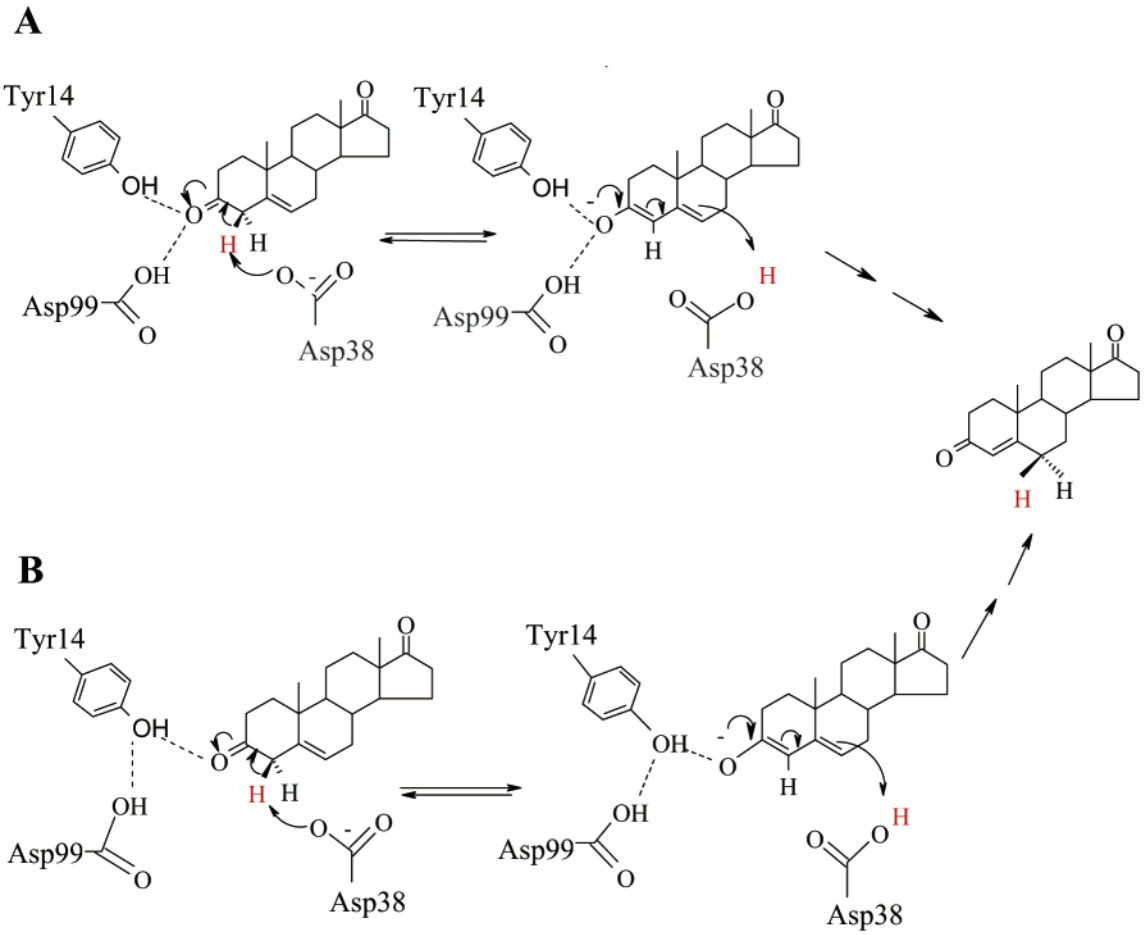

Michaelis complex even in the "so-called" very hydrophobic active site?

By means of X-ray diffraction, NMR, and other spectroscopic studies, as well as site directed mutagenesis, it has been established that Tyr14 and Asp38 are two catalytically critical residues. Besides these residues, Asp99 has been shown to be essential for catalytic activity.[9] The pattern of hydrogen bonding between the steroid and the active site of KSI is a controversial issue (Scheme 2). There is much debate about the precise role of Tyr14 and Asp99 residues. Scheme 2A shows the cooperative hydrogen bond mechanism where both Tyr14 and Asp99 are hydrogen bonded to the O3 of the steroid. This mechanism is supported by X-ray crystallographic studies by Oh and co-workers.[10,11] An important evidence for the cooperative mechanism is the additivity of the effects of mutations at Tyr14 and Asp99.[12] The mechanism shown in Scheme 2B represents the catalytic diad mechanism involving a hydrogen bond between Tyr14 and the O3 of the substrate. The proposed role of Asp99 is to strengthen the hydrogen bond between Tyr14 and steroid O3 by hydrogen bonding to OH of Tyr14. Formation of LBHB has been proposed by Cleland as a general mechanism for many enzyme-catalyzed enolization reactions.[5,13] It has been proposed that LBHB exists between the hydroxylic group of Tyr14 and O3 of the steroid in the KSI catalyzed reaction based on the pK_a matching of the two atoms.[5] The catalytic diad mechanism is supported by the loss of hydrogen bonded proton resonance of both Ty14 and Asp99 in the Tyr14Phe mutant[14] as reported in the elegant NMR studies by Mildvan and co-workers. Mildvan group has also proposed a LBHB between Tyr14-OH and O3 of the steroid.[15,16] Apart from these three residues, Phe101 has also been identified as an important residue (270-fold reduction in k_{cat} in the mutant Phe101Ala, K_m unchanged).[17,18]

A recent paper from the Åqvist group presents a clever theoretical study of the KSI reaction, which unveils the importance of a water molecule in the active site.[19,20] Åqvist et al. use an empirical valence bond (EVB) approach to predict that the hydrogen bond between Tyr14 and steroid O3 cannot be considered a LBHB. Their calculated energetics matches well with the experimental results[21] for the first step of the reaction using a water molecule in the active site, whereas the energetics

(9) Thornburg, L. D.; Henot, F.; Bash, D. P.; Hawkinson, D. C.; Bartel, S. D.; Pollack, R. M. *Biochemistry* **1998**, *37*, 10 499.
(10) Kim, S. W.; Cha, S.-S.; Cho, H.-S.; Kim, J.-S.; Ha, N.-C.; Cho, M.-J.; Joo, S.; Kim, K. K.; Choi, K. Y.; Oh, B.-H. *Biochemistry* **1997**, *36*, 14 030.
(11) Choi, G.; Ha, N.-C.; Kim, S. W.; Kim, D.-H.; Park, S.; Oh, B.-H.; Choi, K. Y. *Biochemistry* **2000**, *39*, 903.
(12) Pollack, R. M.; Thornburg, L. D.; Wu, Z. R.; Summers, M. F. *Arch. Biochem Biophys.***1999**, *370*, 9.
(13) Gerlt, J. A.; Gassman, P. G. *Biochemistry* **1993**, *32*, 11 943.
(14) Zhao, Q.; Abeygunawardana, C.; Gittis, A. G.; Mildvan, A. S. *Biochemistry* **1997**, *36*, 14 616.
(15) Mildvan, A. S.; Massiah, M. A.; Harris, T. K.; Marks, G. T.; Harrison, D. H. T.; Viragh, C.; Reddy, P. M.; Kovach, I. M. *J. Mol. Struct.* **2002**, *615*, 163.
(16) Zhao, Q.; Abeygunawardana, C.; Talalay, P.; Mildvan, A. S. *Proc. Natl. Acad. Sci. U.S.A.* **1996**, *93*, 8220.
(17) Brothers, P. N.; Blotny, G.; Qi, L.; Pollack, R. M. *Biochemistry* **1995**, *34*, 15 453.
(18) Qi, L.; Pollack, R. M. *Biochemistry* **1998**, *37*, 6760.
(19) Feierberg, I.; Åqvist, J. *Biochemistry* **2002**, *41*, 15 728.
(20) Feierberg, I.; Åqvist, J. *Theor. Chem. Acc.* **2002**, *108*,71.

were not well reproduced for the second step in the presence of the same water molecule. In another computational study by the Merz group, both the cooperative hydrogen bond as well as the catalytic diad mechanism were found possible.[22]

In this work, we have used classical molecular dynamics (MD) in combination with periodic boundary conditions to investigate the catalytic mechanism of the KSI reaction. MD simulation of the Enzyme·Substrate (E·S) and the Enzyme·Intermediate (E·In) complexes were carried out for 1500 picoseconds using the NMR solution structure[23] as the starting point and TIP3P explicit solvent model.

Methods

MD Setup. The starting coordinates of the inhibitor-bound TI ketosteroid isomerase homodimer (125 amino acid residues in each subunit) were taken from the published NMR structure, PDB ID: 1BUQ, in the Protein Data Bank.[23] MD simulation of Enzyme·Substrate (E·S) and Enzyme·Intermediate (E·In) complexes were carried out for 1500 picoseconds using the academic version of program CHARMM (version c25b2).[24] Aspartate, glutamate, arginine and lysine residues were charged and all the tyrosine residues were neutral unless otherwise specified. Asp99-CO_2H was neutral in MD simulations of E·S and E·In. In the MD simulation of E·S, Asp38 (general base, Asp38-CO_2^-) was negatively charged whereas in E·In, Asp38 (general acid, Asp38-CO_2H) was neutral with a proton (HD2) on OD2.

The enzyme being a homo-dimer allowed substrate to be modeled in the first active site and the intermediate in the second active site. Since the enzyme follows Michaelis−Menten kinetics,[25,26] there is no allosteric effect between the subunits. The enzyme−substrate−intermediate system was solvated in an equilibrated TIP3P water box of dimension 65 Å × 59 Å × 53 Å using the center of mass of the enzyme as the origin. Any solvent molecule within 2.8 Å of a heavy atom of the enzyme was deleted.

The solvent molecules (19524 atoms) were minimized and equilibrated at 300 K for 3 ps keeping the protein, ligand and the crystallographic water molecules fixed to allow favorable distribution of water molecules on the enzyme surface. Before the start of the dynamics, the enzyme−substrate−intermediate systems were energy minimized using the steepest descents (SD) method followed by adopted basis Newton−Raphson (ABNR) method.

The CHARMM 27 residue topology and parameter file were used for protein atoms and the ligands. Some of the torsional parameters for the ligand were unavailable in CHARMM and were generated using ab initio (vide infra). Periodic boundary conditions were used to perform the MD simulation. The SHAKE algorithm[27] was used to constrain the bonds containing hydrogens to their equilibrium length. The Verlet leapfrog algorithm was used to integrate the equations of motion.[28] Molecular dynamics simulations were carried out at constant pressure and temperature for 1.5 nanoseconds using an integration time step of 0.0015 ps. The nonbonded list was updated every 20 time steps, and the nonbonded interactions were cut off at 12 Å. The Coulombic term was cut off by using a force-shifting function, and the Lennard−Jones term was cut off with a switching function. The system was initially coupled to a 200 K heat bath for 15 ps by using a coupling constant of 5.0 ps. The system was subsequently coupled to a heat bath at 300 K for the rest of the simulation by using a coupling constant of 5.0 ps. The pressure was constantly maintained by a Berendsen algorithm using an isothermal compressibility of 4.63×10^{-5} atm^{-1} and a pressure coupling constant of 5.0 ps.[29] Coordinates from the MD simulation were saved every 100 time steps.

The last 1100 ps of trajectory were used for analysis and reporting the average structure. To identify hydrogen bonds, distances between H-bond donor and acceptor were determined. Structures where the H···O distance was ≤1.9 Å were considered hydrogen-bonded. Covariance matrix was calculated to determine the extent of correlated motion between the α-carbons of the residues and plotted with GMT.[30] The initial (before starting MD) and final dimensions of the water box were 66.4 Å × 58.0 Å × 52.9 Å and 67.0 Å × 56.8 Å × 53.5 Å, respectively.

Preliminary calculations were carried out on SGI Origin 2000 at UC Santa Barbara Supercomputing Facility, GUASSIAN98[31] calculations were done on SGI Origin 2000 at University of Illinois at Urbana-Champaign (NCSA) and molecular dynamics simulations were performed on a CRAY T3E (NPACI) platform at University of Texas Supercomputing Center at Austin.

Parameters for Molecular Dynamics. The standard CHARMM force field does not have parameters to describe torsional modes of the bound substrate or intermediate. To determine values for missing torsional parameters, conformational analysis with quantum mechanical methods were performed with a set of model compounds. These conformational energies were then calculated with CHARMM and parameter values were adjusted until a good agreement between CHARMM results and ab initio data was obtained. The set of model compounds, shown in Chart 1, includes butanal (1), 3-butenal (2), anion of 3-butenal (3), 4-penten-2-one (4), 3-methylenecyclohexanone (5), 4,4-dimethyl-3-methylene-cyclohexanone (6), and 3,4,4a,5,6,7-hexahydro-4a-methyl-2(1H)-naphthalenone (7).

Detailed conformational analysis of 3-butenal was carried out at the MP2/aug-cc-pVTZ//MP2/cc-pVTZ level with Gaussian98.[31] Possible conformations of 3-butenal arise from rotations around the OC−CC and CC−CC dihedrals. Three minima were identified for this molecule. The gauche$^+$-gauche$^+$ structure with the OC−CC dihedral at 113.4° and the CC−CC dihedral at 107.1° was the global minimum; the two local minima (syn-gauche$^+$ and gauche$^+$-gauche$^-$) were 0.19 and 0.44 kcal/mol higher in energy. Full torsional energy profiles for 3-butenal are given in Supporting Information (Figure S1). The anion of 3-butenal had two planar minimum energy structures. The conformer with OC−CC at 180° was the global minimum and the conformer with CC−CC at 0° was higher in energy by 1.4 kcal/mol. Two minima were located on the potential energy surface for 4-penten-2-one. The gauche$^-$-gauche$^+$ structure with C−C−C−C dihedral at −86.8° and C−C−C═C dihedral at 114.0° was global minimum. The anti-gauche conformer with C−C−C−C dihedral at −165.8° and C−C−C═C dihedral at 128.6° was 0.46 kcal/mol less stable at the MP2/aug-cc-pVTZ//MP2/cc-pVTZ level. Compounds 5 and 6 can adopt either a chair or a twist-boat conformation. The chair form was found to be the most stable, and the energy gap between the two forms was 2.81 kcal/mol and 1.73 kcal/mol at the MP2/cc-pVTZ level for 3-methyl-

(21) Hawkinson, D. C.; Eames, T. C. M.; Pollack, R. M. *Biochemistry* **1991**, *30*, 10 849.
(22) Park, H.; Merz, K. M., Jr. *J. Am. Chem. Soc.* **2003**, *125*, 901.
(23) Massiah, M. A.; Abeygunawardana, C.; Gittis, A. G.; Mildvan, A. S. *Biochemistry* **1998**, *37*, 14 701.
(24) Brooks, B. R.; Bruccoleri, R. E.; Olafson, B. D.; States, D. J.; Swaminathan, S.; Karplus, M. *J. Comput.Chem.* **1983**, *4*, 187.
(25) Kim, S. W.; Choi, K. Y. *J. Bacteriol.* **1995**, *177*, 2602.
(26) Xue, L.; Talalay, P.; Mildvan, A. S. *Biochemistry* **1990**, *29*, 7491.
(27) Ryckaert, J. P.; Ciccotti, G.; Berendsen, H. J. C. *J. Comput. Phys.* **1977**, *23*, 327.
(28) Verlet, L. *Phys. Rev.* **1967**, *169*, 98.
(29) Berendsen, H. J. C.; Postma, J. P. M.; Van Gunsteren, W. F.; DiNola, A.; Haak, J. R. *J. Chem. Phys.***1984**, *81*, 3684.
(30) Wessel, P.; Smith, W. H. F. *EOS Trans. AGU* **1998**, *79*,579.
(31) Frisch, M. J.; Trucks, G. W.; Schlegel, H. B.; Scuseria, G. E.; Robb, M. A.; Cheeseman, J. R.; Zakrzewski, V. G.; Montgomery, J. A.; Stratmann, R. E.; Burant, J. C.; Dapprich, S.; Millam, J. M.; Daniels, A. D.; Kudin, K. N.; Strain, M. C.; Farkas, O.; Tomasi, J.; Barone, V.; Cossi, M.; Cammi, R.; Mennucci, B.; Pomelli, C.; Adamo, C.; Clifford, S.; Ochterski, J.; Petersson, G. A.; Ayala, P. Y.; Cui, Q.; Morokuma, K.; Malick, D. K.; Rabuck, A. D.; Raghavachari, K.; Foresman, J. B.; Cioslowski, J.; Ortiz, J. V.; Stefanov, B. B.; Liu, G.; Liashenko, A.; Piskorz, P.; Komaromi, I.; Gomperts, R.; Martin, R. L.; Fox, D. J.; Keith, T.; Al-Laham, M. A.; Peng, C. Y.; Nanayakkara, A.; Gonzalez, C.; Challacombe, M.; Gill, P. M. W.; Johnson, B.; Chen, W.; Wong, M. W.; Andres, J. L.; Gonzalez, C.; Head-Gordon, M.; Replogle, E. S.; Pople, J. A. *GAUSSIAN 98*; Guassian, Inc.: Pittsburgh, PA, 1998.

Chart 1

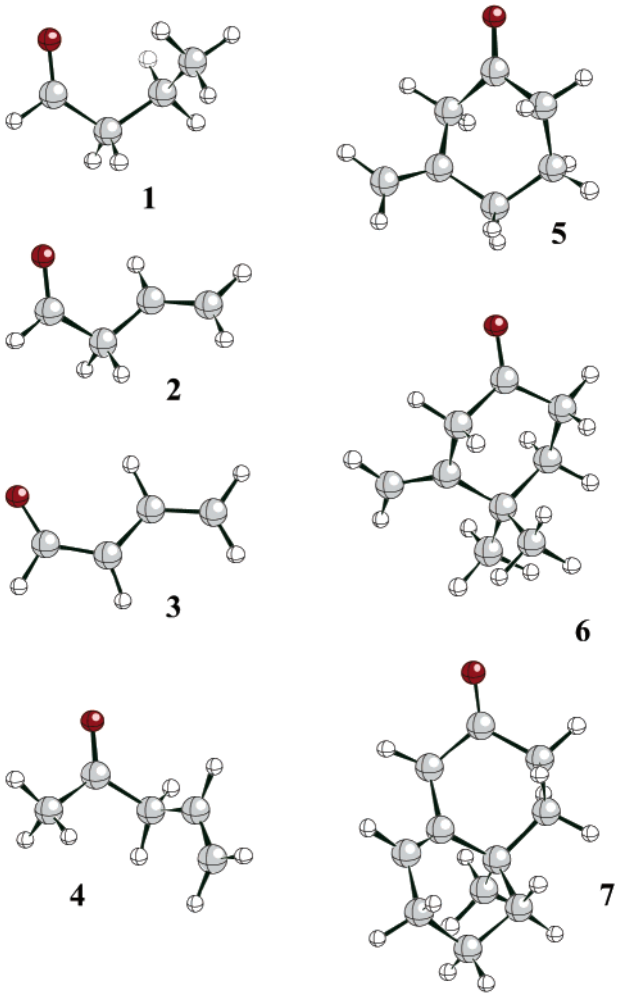

enecyclohexanone and 4,4-dimethyl-3-methylene-cyclohexanone, respectively. The chair conformer was 1.31 kcal/mol below the twist-boat conformer in 3,4,4a,5,6,7-hexahydro-4a-methyl-2(1H)-naphthalenone at MP2/6-311+G(2d,p) level.

Models 2 and 3 were used to calculate the charge distribution of the ketone and enolate function in the substrate and intermediate, respectively. The electrostatic potentials were obtained from the MP2/6-311+G(2d,p) optimized geometry of 2 and 3 using the Merz−Kollman scheme implemented in Guassian98.[32] RESP fitting of the point charges to these electrostatic potentials was done to obtain the charges for the model compound.[32,33] On the basis of our MP2/RESP calculation, the charge of O3 in substrate and intermediate were −0.50 eu and −0.65 eu, and the charge of C3 in substrate and intermediate were 0.59 and 0.40 eu. The standard CHARMM charges were used for the rest of the atoms.

Results

Stability of Trajectory. The molecular dynamics simulations of solvated E·S and E·In systems were carried out for 1.5 nanoseconds. As a measure of structural stability, root-mean-square deviations (RMSD) from the starting structure were calculated on the basis of superposition of all the backbone heavy atoms of E·S (Figure 1A) and E·In (Figure 1B) systems. After an initial increase during heating and equilibration period for the first 200 picoseconds, a plateau is reached. As shown in Figure 1, the average RMSD for the backbone (excluding hydrogen atoms) is 1.5 ± 0.16 Å for E·S simulation. The corresponding value for E·In simulation is 1.6 ± 0.14 Å respectively. After 200 ps, the values fluctuate very little, indicating a stable and equilibrated protein structure. The atom numbering scheme for substrate and intermediate is shown in Scheme 1. The distances discussed in the following sections are shown in Table 1.

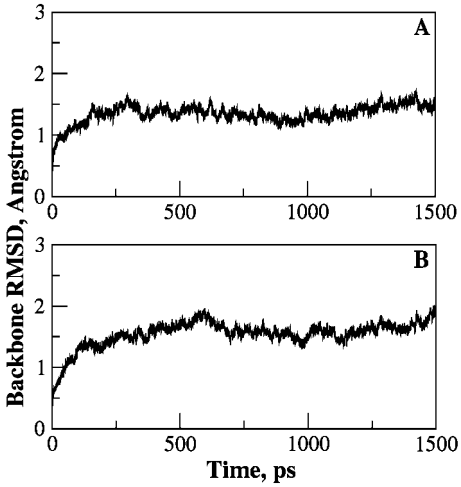

Figure 1. Time dependence of backbone RMSD in E·S **(A)** and E·In **(B)** during 1.5 ns MD simulation.

Table 1. Average Distances during MD Simulation of E·S and E·In[a]

	distance from E·S	distance from E·In
Tyr14 OH····O3	3.1 ± 0.4	2.7 ± 0.1
Asp99 OD2····O3	2.7 ± 0.2	2.8 ± 0.2
Phe86 CZ····O17	3.3 ± 0.3	3.7 ± 0.7
Tyr14 OH····Tyr55 OH	3.0 ± 0.3	2.9 ± 0.2
Asp38 OD2····H_β(C4)	2.8 ± 0.4	
Asp38 OD2····H_α(C4)	3.1 ± 0.2	
Asp38 OD2····C4		3.7 ± 0.4
Asp38 OD2····C6		3.5 ± 0.2
Asp38 OD1····Wat6055	2.7 ± 0.1	
Tyr14 OH····Wat6055	4.2 ± 0.8	
Phe82 CZ····C3	3.7 ± 0.3	3.3 ± 0.2
Val84 CG1····C1	4.5 ± 0.4	4.3 ± 0.3
Phe116 CZ····C15	4.7 ± 0.6	3.5 ± 0.2
Phe116 CE1····C7	4.2 ± 0.3	4.1 ± 0.2
Val95 CG2····C16	4.2 ± 0.3	4.1 ± 0.3

[a] Distances shown in angstrom.

Results from the MD simulation of E·S. The MD simulation of E·S complex highlights the mode of binding of substrate (androst-5-ene-3,17-dione, Scheme 1) to the active site (Figure 2). For simplicity, the interactions in the active site have been divided into (a) polar, and, (b) nonpolar interactions.

a. Polar Interactions/Hydrogen Bonds in the Active Site. The steroid substrate makes hydrogen bonds using both of the carbonyl oxygens—O3 and O17. The substrate binds to the active site in such a fashion that O3 is buried in the active site whereas O17 is exposed to the solvent (Figure 2). The hydroxylic hydrogen of Tyr14 is hydrogen bonded to O3 of steroid for 31% ($R_{O\cdots H} \leq 1.9$ Å) of time with the average distance of 3.1 ± 0.4 Å ($R_{O3\cdots OH}$) (Figures 2 and 3A). The second hydrogen bond to steroid O3 is made by the acidic hydrogen (HD1) of Asp99-CO_2H (Figures 2 and 3B). This

(32) Besler, B. H.; Merz, K. M. J.; Kollman, P. A. *J. Comput. Chem.* **1990**, *11*, 431.
(33) Bayly, C. I.; Cieplak, P.; Cornell, W. D.; Kollman, P. A. *J. Phys. Chem.* **1993**, *97*, 10 269.

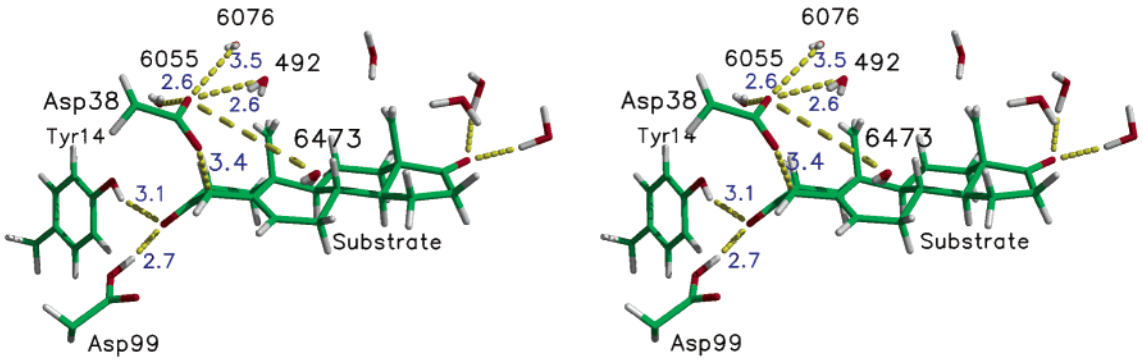

Figure 2. Average (coordinates averaged over the last 1100 ps of MD) structure of the active site during MD simulation of E·S shown in stereo. The distances between the heavy atoms are shown in angstroms. Note the interactions of Tyr14 and Asp99 with O3 of the substrate and hydrogen bonds of Asp38 with solvent waters.

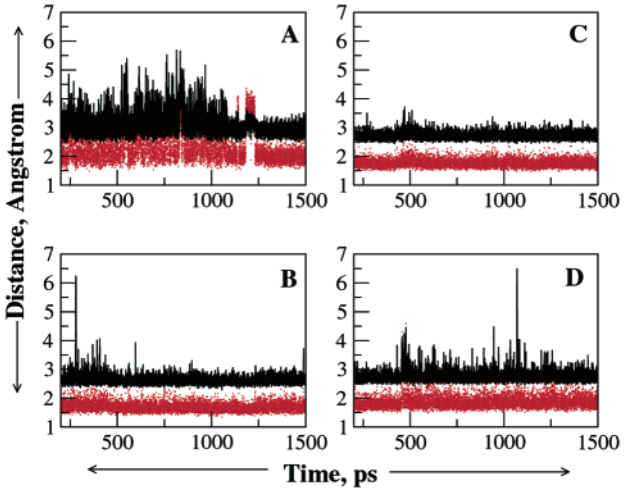

Figure 3. Hydrogen bonds to the O3 of steroid in E·S and E·In complex during 1.5 ns MD simulation. Distance between hydrogen on OH of Tyr14 and O3 of steroid in MD simulations of E·S **(A)** and E·In **(C)**. Distance between hydrogen on carboxylate OD1 of Asp99 and O3 of steroid in the ground state **(B)** and Intermediate state **(D)**. The solid black line shows the heavy atom distance, $R_{O\cdots O}$ and red dotted line shows the distance between the oxygen and hydrogen atom, $R_{O\cdots H}$.

hydrogen bond is present for 80% ($R_{O\cdots H} \leq 1.9$ Å) of time with the average distance of 2.7 ± 0.2 Å ($R_{O3\cdots OD1}$).

The carbonyl O17 of steroid is solvent exposed and is found to make two or three hydrogen bonds to TIP3P waters at any point of time during MD simulation (Figure 2). The O17 of steroid is also found to approach the partially positively charged ring hydrogen atoms of Phe86 (Figure 4) and maintain a stable distance throughout the MD simulation ($R_{CZ\cdots O17} = 3.3 \pm 0.3$ Å). The tyrosine diad, consisting of residues Tyr14 and Tyr55, exhibits a stable hydrogen-bonding pattern during the simulation (Figure 4). The residue Tyr55-OH is hydrogen bonded to Tyr14 for 46% ($R_{O\cdots H} \leq 1.9$ Å) of the time with the average distance of 3.1 ± 0.3 Å ($R_{O\cdots OH}$).

The environment of Asp38-CO_2^- is polar compared to other active site aspartate, Asp99-CO_2H. At any time during the MD simulation, the carboxylate oxygen OD1 of Asp38-CO_2^- is hydrogen bonded to three or four TIP3P water molecules (Figure 2 and also see, Figure 5). Water6055 hydrogen bonds to the OD1 of Asp38-CO_2^- and, occasionally, to the OH of Tyr14 with the average distance 2.7 ± 0.1 Å and 4.2 ± 0.8 Å respectively (Figure 5, parts A and B). At various times, Water425, Water492, Water2074, Water5746, Water6076, and

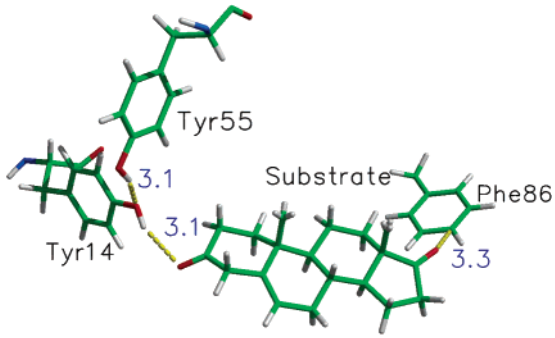

Figure 4. Average structure from the MD simulation of E·S showing the orientation of Phe86 with respect to the substrate. Note the hydrogen bond between Tyr14-OH and Tyr55-HH.

Water6473 are hydrogen bonded to OD1 of Asp38-CO_2^- carboxylate (Figure 5, parts C−H).

b. Nonpolar Interactions. The active site of KSI is predominantly hydrophobic and specifically interacts with the hydrophobic steroid substrate (Figure 6A). The enzymatic residues make favorable contacts with all four rings (A, B, C, and D; see Scheme 1 for the naming of the rings) of the substrate. The residues Leu18, Phe82, Val84, and Ala114 make nonpolar contact with ring A with average distances 4.2 ± 0.7 Å ($R_{CD2\cdots C1}$), 3.7 ± 0.3 Å ($R_{CZ\cdots C3}$), 4.5 ± 0.4 Å ($R_{CG1\cdots C1}$) and 4.9 ± 0.4 Å ($R_{CB\cdots C4}$), respectively. The aromatic ring of Phe116 interacts favorably with both rings B and D with the average distance of 4.2 ± 0.3 Å ($R_{CE1\cdots C7}$) and 4.7 ± 0.6 Å ($R_{CZ\cdots C15}$). The side chain of Val95 interacts with ring D at an average distance of 4.2 ± 0.3 Å ($R_{CG2\cdots C16}$). The residue Asp99-CO_2H is surrounded by Tyr14, Phe80, Phe82, Phe101, Met112, Ala114 and Pro297 throughout the MD simulation.

Results from the MD simulation of E·In. MD simulation of E·In highlights the mode of binding of the intermediate (3-hydroxy-androsta-3,5-dien-17-one, Scheme 1) of the KSI reaction (Figure 7). The interactions in the active site have been divided into (a) polar, and, (b) nonpolar interactions.

a. Polar Interactions/Hydrogen Bonds in the Active Site. The interactions of both the intermediate and substrate with KSI active site are very similar. The enolate O3 of intermediate is embedded in the active site whereas the carboxyl O17 is exposed to the solvent (Figure 7). The hydrogen on OH of Tyr14 is hydrogen bonded to O3 of intermediate for 94% ($R_{O\cdots H} \leq 1.9$ Å) of time with the average distance of 2.7 ± 0.1 Å ($R_{O3\cdots OH}$; Figure 3C). The second hydrogen bond to the O3 of the intermediate is made by the acidic hydrogen (HD1) of Asp99-

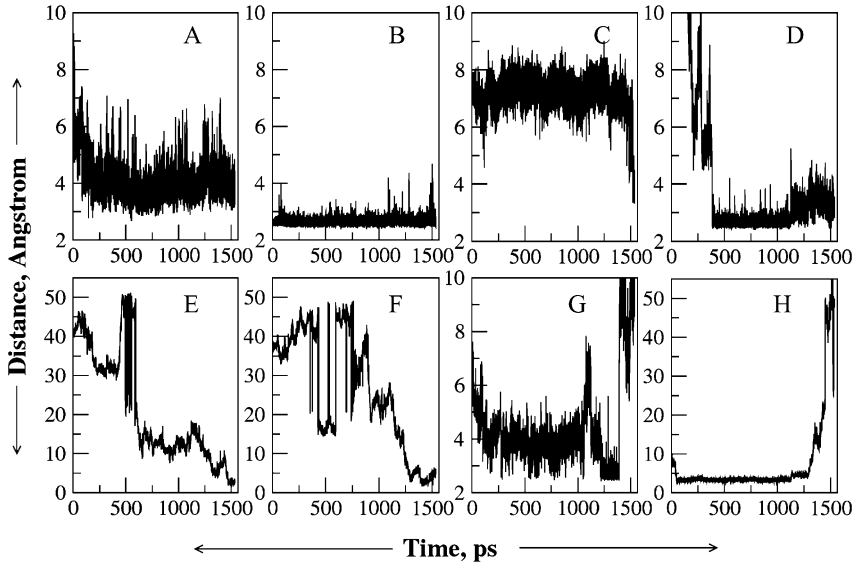

Figure 5. Interactions of Asp38 carboxylate (OD1) and Tyr14 (OH) with water during MD simulation of E·S. The figure shows the time dependent motion of various waters in the active site. The *Y*-axis shows the distance between heavy atoms in Angstroms and *X*-axis shows the time in picoseconds. Hydrogen bonding distance plotted between (A) Tyr14 OH···Wat6055, (B) Asp38 OD1···Wat6055, (C) Asp38 OD1···Wat425, (D) Asp38 OD1···Wat492, (E) Asp38 OD1···Wat5746, (F) Asp38 OD1···Wat2074, (G) Asp38 OD1···Wat6076, and (H) Asp38 OD1···Wat6473.

CO_2H (Figure 3D). This hydrogen bond is present for 75% ($R_{O\cdots H} \leq 1.9$ Å) of time with the average distance of 2.8 ± 0.2 Å ($R_{O3\cdots OD1}$).

The carbonyl O17 of intermediate is solvent exposed and is hydrogen bonded to TIP3P waters throughout the MD simulation (Figure 7). The O17 of intermediate is also found to approach the partially positively charged ring hydrogen atoms of Phe86 throughout the MD simulation ($R_{CZ\cdots O17} = 3.7 \pm 0.7$ Å).

The hydrogen bonding in the tyrosine diad, consisting of the residues Tyr14 and Tyr55, is stable during the simulation (Figure 7). The hydroxyl (OH) of Tyr55 is hydrogen bonded to Tyr14 OH for 72% ($R_{O\cdots H} \leq 1.9$ Å) of the time with the average distance of 2.9 ± 0.2 Å ($R_{O\cdots OH}$). The bulky phenyl ring of Phe101 is adjacent to the tyrosine diad, Tyr14 and Tyr55. The partially positively charged ring hydrogens of Phe101 point toward the phenyl ring of Tyr14 with the interplanar angle of 70 degrees throughout the MD simulation (Figure 7).

The OD2 of the general acid Asp38-CO_2H is at a distance 3.5 ± 0.2 Å and 3.7 ± 0.4 Å from the C6 and C4 of the intermediate, respectively (Figures 7 and 8, parts A and B). The angle of attack between Asp38-CO_2H and the intermediate is measured as the angle between carboxylic OD2, proton HD2 of Asp38-CO_2H and atom C6 or C4 of intermediate. The attack angle to C6 and C4 of the intermediate are shown in Figure 8C and 8D, respectively. The carboxyl oxygens of Asp38-CO_2H do not make any contact with the solvent water throughout the MD simulation of E·In.

b. Nonpolar Interactions. The interactions between the intermediate and the hydrophobic active site residues are shown in Figure 6B. The residues Leu18, Phe82, Val84, and Ala114 make nonpolar contact with ring A (see Scheme 1 for the naming of the rings) with average distance of 4.2 ± 0.7 Å ($R_{CD2\cdots C1}$), 3.3 ± 0.2 Å ($R_{CZ\cdots C3}$), 4.3 ± 0.3 Å ($R_{CG1\cdots C1}$), and 4.3 ± 0.4 Å ($R_{CB\cdots C4}$), respectively. The aromatic ring of Phe116 interacts favorably with both B and D rings with the average distance of 4.1 ± 0.2 Å ($R_{CE1\cdots C7}$) and 3.5 ± 0.2 Å ($R_{CZ\cdots C15}$). The side chain of Val95 interacts with ring D with average distance of 4.1 ± 0.3 Å ($R_{CG2\cdots C16}$). The hydroxyl side chain of Ser58 interacts with the methyl groups at C18 and C19 with average distance of 4.0 ± 0.4 Å ($R_{OG\cdots C18}$) and 4.1 ± 0.5 Å ($R_{OG\cdots C19}$). The phenyl group of Phe54 interacts with the C19 methyl with the average distance of 4.0 ± 0.5 Å ($R_{CZ\cdots C19}$). Asp99-CO_2H is well surrounded by the residues Tyr14, Phe80, Phe82, Phe101, Met112, Ala114, and Pro297.

Atomic Motions during the MD Simulation of E·S and E·In. Analysis of correlation of atomic motions revealed that several residues moved in a concerted manner. Correlation plots generated from the MD simulation of E·S and E·In are shown in Supplemental Figure S2. The β-sheets show correlated motion and manifests itself as set of parallel lines on the correlation motion plot. Almost all the residues that are positively correlated during the MD simulation of E·S showed a similar correlation pattern during E·In MD simulation. The active site residues Asp38 and Tyr14 show negative correlation for 5% of time in E·S and 23% of time in E·In. The extent of anticorrelation between the residues Tyr14 and Asp38 using Val84 as the reference point is shown in Figure 9. The residue Val84 is chosen as the reference point based on its location relative to Tyr14 and Asp38. The individual time series of the Tyr14-Val84 and Asp38-Val84 distances are shown in Supporting Information, Figure S3.

Discussion

Ketosteroid isomerase (KSI) catalyzes the steroid transformation, shown in Scheme 1, at a rate approaching the diffusion controlled limit ($k_{cat}/K_m = 3.0 \times 10^8$ M^{-1} s^{-1}). Despite the extensive kinetic and structural work, there are some gaps in understanding the mechanism and role of different active site residues of KSI. Two mechanisms have been proposed to account for the precise role of the residues Tyr14 and Asp99. They are: (i) the cooperative hydrogen bond mechanism, where both Tyr14-OH and Asp99-CO_2H are hydrogen bonded to the O3 of the steroid (Scheme 2A), and, (ii) the catalytic diad mechanism, where only Tyr14-OH is hydrogen bonded to the O3 oxygen of steroid with assistance from the hydrogen bond between HD2 of Asp99-CO_2H and Tyr14-OH (Scheme 2B).

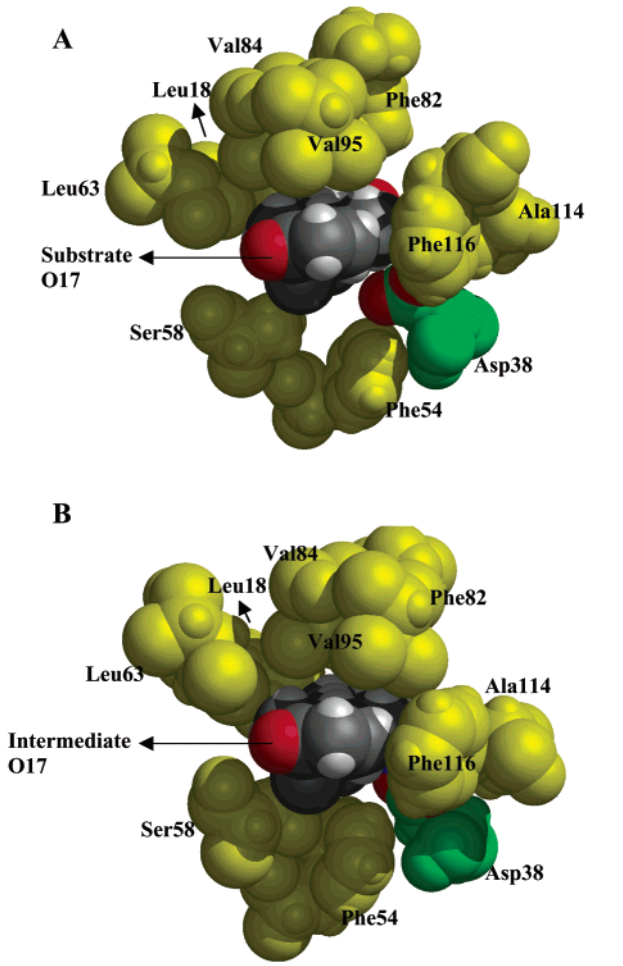

Figure 6. Average structure from the MD simulation showing the nonpolar interactions between the ligand and the active site. All the hydrophobic residues are shown in yellow. All atoms of Asp38 are shown in green with the carboxylate oxygens in red. Color scheme for Ligand: Grey for carbon, red for oxygen and white for hydrogen. **(A)** Interaction between the steroid and the active site residues obtained from MD simulation of E·S. **(B)** Interaction between the intermediate and the active site residues obtained from MD simulation of E·In. Note the environment of Asp38 in A and B. The carboxylate of Asp38 is more exposed in E·S (A) compared to E·In (B). The hydrophobic residues form a closed structure around Asp38 in E·In (B), restricting the entrance of water in the active site.

MD simulations were carried out on enzyme-bound substrate (E·S) and intermediate (E·In) using TIP3P water as a solvent to hydrate the system (Scheme 1). The starting coordinates were taken from the published NMR structure of Δ^5-3-ketosteroid isomerase complexed with the steroid 19-nortestosterone hemisuccinate from the species *Pseudomonas testosteroni*.[23] In the MD simulation of E·S, Asp38 (general base, Asp38-CO_2^-) is negatively charged, whereas in E·In, Asp38 (general acid, Asp38-CO_2H) is neutral with a proton (HD2) on OD2. On the basis of its location in the hydrophobic pocket and experimental evidence,[16] Asp99 is neutral (Asp99-CO_2H) in both E·S and E·In.

Our molecular dynamics results support the cooperative hydrogen bond mechanism (Scheme 2A) wherein both Tyr14-OH and Asp99-CO_2H are hydrogen bonded to the O3 oxygen of the steroid (Figure 2) and intermediate (Figure 7). The starting coordinates for our MD simulation were taken from the NMR structure,[23] wherein Tyr14-OH is hydrogen bonded to the O3 of steroid and Asp99-CO_2H is hydrogen bonded to Tyr14 (Figure 10). This NMR structure was used by Mildvan et al. to support the catalytic diad mechanism (Scheme 2B). What is not immediately obvious, however, is the fact that this NMR structure was obtained by using a distance constraint of 2.45 ± 0.15 Å between Asp99-CO_2H and Tyr14-OH in the structure calculations.[23] Interestingly, when this constraint is removed in a "control" computation by Mildvan et al., the distance between Asp99-CO_2H and Tyr14-OH increases to 3.98 ± 0.55 Å, consistent with the cooperative hydrogen bond mechanism, similar to our results. On initiation of minimization step, the proton (HD2) on carboxylic of Asp99-CO_2H orients in a direction that prefers hydrogen bonding to the O3 oxygen atom of substrate rather than OH of Tyr14 (Figure 2). The phenolic OH of Tyr14 is also hydrogen bonded to the carbonyl oxygen O3 of the substrate with the average distance of 3.1 ± 0.4 Å. The hydrogen bond between OH of Tyr14 and O3 exhibits less fluctuation and a shorter distance (2.7 ± 0.1 Å) in the intermediate (compare Figure 3, parts A and B), which suggests that this hydrogen bond might be stronger in the intermediate than in the substrate. The average hydrogen bonding distances between Tyr14-OH and O3 in the substrate and intermediate were compared using the t-statistics and the calculated t-value showed that there is a statistical difference between the two averages at a confidence level of 95%. Thus, Tyr14 plays a crucial role in the preferential stabilization of the dienolate intermediate. Due to force-field limitations, it is not possible to judge the existence of a LBHB bond by MD simulation. However, presence of a strong hydrogen bond, possibly of a LBHB, cannot be ruled out considering the following observations:[5] (i) the hydrogen bond between the residues Tyr14-OH and O3 becomes stronger in E·In complex with the average distance of 2.7 ± 0.1 Å, (ii) water squeezed out (low dielectric environment) from the active site in E·In complex (vide infra). Hence, our MD simulation strongly supports the cooperative hydrogen bond mechanism (Scheme 2A) rather than the catalytic diad mechanism (Scheme 2B, also see Figure 10).

The hydrophobic residues in the active site of KSI make a cage that fits the substrate well (Figure 6A). The hydrophobic side chains of the residues Leu18, Phe82, Val84, Val95, Ala114, and Phe116 make favorable contacts with all the four rings of the substrate. The bulky side chains play an important role in maintaining a hydrophobic active site by shielding from solvent entrance. The fact that the pK_{app} of Asp38 in the Michaelis complex is 4.75[8] in the "so-called" very hydrophobic active site of KSI, is very intriguing. It might be supposed that the pK_a of Asp38 would be raised in a hydrophobic environment. If this were so the general base Asp38-CO_2^- would not be present to catalyze the first step of steroid to intermediate conversion. This anomaly can be explained by the hydrogen bonding of Asp38-CO_2^- to solvent water, as shown by our MD simulation of E·S and E·In (Figure 2). During MD simulation of E·S, Asp38-CO_2^- maintains two or three hydrogen bonds to the solvent water. These hydrogen bonds and access to the solvent water pool helps to keep the pK_{app} of Asp38 close to its pK_a in water. Such water molecules were not identified in any of the published X-ray and NMR structures. However, X-rays failing to detect water molecules is not very unusual.[34] The solvent waters, Wat425, Wat492, Wat5746, Wat2074, enter the active site

(34) Ernst, J. A.; Clubb, R. T.; Zhou, H. X.; Gronenborn, A. M.; Clore, G. M. *Science* **1995**, *267*, 1813.

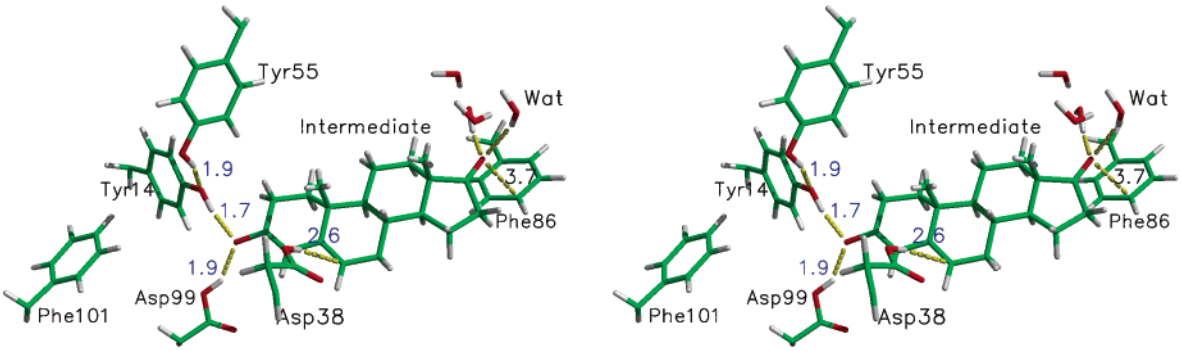

Figure 7. Stereoplot showing the average active site structure of KSI during the MD simulation of E·In. The distance between O···H is shown in Angstrom. The figure shows the hydrogen bond between Tyr14-O3, Asp99-O3, Tyrosine diad Tyr14-Tyr55 in the intermediate step. Note the orientation of Phe86 and Phe101. The O17 of intermediate is solvent exposed. Also, note the favorable geometry of proton (HD2) on Asp38 for attack on C6 of intermediate.

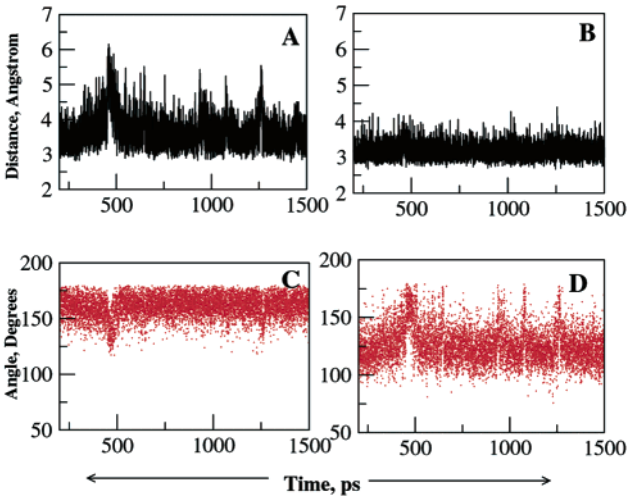

Figure 8. Distance between OD2 of Asp38 and atom C6 **(A)** or C4 **(B)** of the intermediate. The angle of attack between Asp38-CO_2H and the C6 of intermediate **(C)**, or, the C4 of intermediate **(D)**. The attack angle of Asp38 is measured as angle between carboxylate OD2, proton HD2 of Asp38 and C6 or C4 of the intermediate.

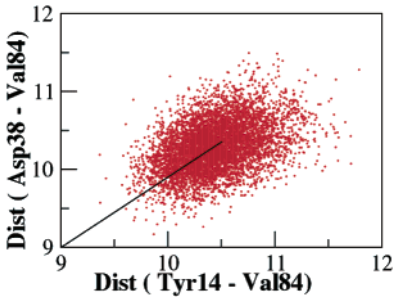

Figure 9. Anticorrelation between the residue Tyr14 and Asp38 using Val84 as the reference during MD simulation of E.In. Val84 chosen as the reference point because it is equidistant from both Tyr14 and Asp38 and shows very little motion during MD simulation. Note the strong anti-correlation between Tyr14 and Asp38.

during MD simulation of E·S, whereas Wat6076 and Wat6473 move out from the active site. The solvent water, Wat6055, occupies a position such that it can hydrogen bond to OD1 of Asp38-CO_2^- and, occasionally, to OH of Tyr14 at the same time. This structure is maintained during the MD simulation of E·S. In the Åqvist simulation,[19] it was shown that presence of such a water molecule is required to reproduce the experimental free energy for the first step of the reaction, whereas the energetics were not well reproduced for the second step in the presence of the same water molecule. The simulation was,

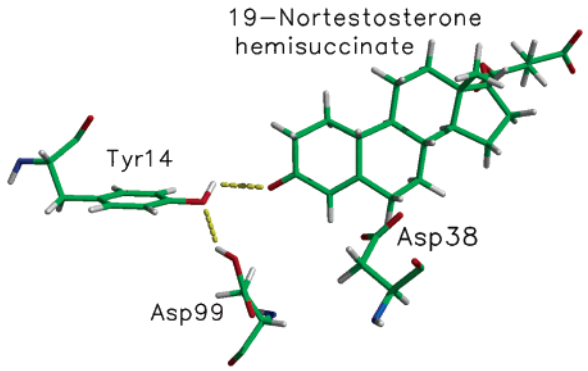

Figure 10. Starting structure for MD simulation: NMR structure showing the hydrogen bond between Asp99 and Tyr14. Note that Tyr14 alone donates a hydrogen bond to the O3 of the substrate.

however, performed with KSI from PI. Our MD simulation, performed on KSI from TI, clearly shows that such a water molecule is present only in the E·S complex. In the structures obtained from the MD simulation of E·In, the active site hydrophobic residues have moved closer to the intermediate and shield Asp38-CO_2H from solvent water (compare Figure 6, parts A and B). In doing so the pK_{app} of Asp38-CO_2H is increased and the general acid is stabilized.

One might ask the question as to how does a water molecule enter the active site of KSI in the E·S complex? A possible explanation to this question can be attributed to the position of the hydrophobic residues that guard the active site (Figure 6, parts A and B). Especially, the residues Phe54, Ser58, Ala114, and Phe116 tend to move closer to the intermediate compared to substrate. It is clearly visible from Figures 6A and 6B that the active site is more "closed" in the E·In complex than in the E·S complex. The hydrophobic residues can possibly shield water from entering the active site, thus playing an important role in controlling the dynamics of water in the active site.

It has been observed that KSI only slightly favors protonation of the intermediate at C-4, despite the fact that in solution protonation of the intermediate is favored at C-4 by about 2 kcal/mol.[35] Our MD simulation of E·In also supports this observation. The OD2 of Asp38-CO_2H is at a distance 3.2 ± 0.2 Å ($R_{HD2\cdots C4}$ = 2.5 ± 0.2 Å) and 3.5 ± 0.5 Å ($R_{HD2\cdots C6}$ = 2.6 ± 0.5 Å) from C4 and C6 of the intermediate, respectively (Figure 8). The angle of proton donation at C6 (∠Asp38-OD2····HD2·····Intermediate-C6 = 166.2 ± 10°) is more

(35) Zeng, B.; Pollack, R. M. *J. Am. Chem. Soc.* **1991**, *113*, 3838.

favorable compared to that for C4 (∠Asp38-OD2····HD2····· Intermediate-C4 = 125.6 ± 15°). Although both C4 and C6 have almost similar distance from proton (HD2) on the carboxylic OD2 of Asp38-CO_2H, this favorable angle of approach orients HD2 of Asp38-CO_2H toward the C6 of intermediate. Thus, even though the difference in protonation of C6 and C4 is not large from the point of distance between the two reacting atoms, the residue Asp38-CO_2H plays a crucial role by distinguishing the two carbons by orienting its proton toward C6.

The drop in k_{cat} on mutation of Phe101 to Ala or Leu can be also explained on the basis of our MD simulations.[17,18] The bulky phenyl ring of Phe101 fits in the cavity adjacent to the tyrosine diad, Tyr14 and Tyr55, and the partially positively charged ring hydrogens of Phe101 point toward the phenol ring of Tyr14 with the interplanar angle of 70 degrees throughout the MD simulation (Figure 7). Similar interactions have been reported for protein structure stabilization and classified as weakly polar interaction in the literature.[36] The interaction energy between phenol and benzene model using the average structure from our MD simulation of E·In and the MP2/6-31+G(d,p) level of theory gave a value of −3.8 kcal/mol in the gas phase. Mutating the residue Phe101 to a less bulky group will hinder this favorable interaction with Tyr14. Moreover, the motion of Tyr14 will be very floppy without the rigid support from Phe101.

Analysis of correlation of atomic motions from the MD simulation of E·S and E·In reveal that there is an anticorrelated motion between the catalytically critical residues, Tyr14 and Asp38 (Figure 9). The anticorrelation motion can be defined as the motion of Asp38 and Tyr14 toward each other. This motion is present for 5% of time in E·S and 23% of time in E·In. Asp38-CO_2^- can abstract the proton from C4 with the assistance from the Tyr14-OH hydrogen bonding to the O3 oxygen of steroid at the same time. Thus, the anticorrelated motion between Tyr14 and Asp38 might be considered as a promoting motion for KSI catalysis and a possible subject for further investigations.

Conclusions

KSI catalyzes proton abstraction from the C−H function adjacent to carbonyl or carboxyl group at a rate approaching diffusion limit. Two alternative mechanisms that have been proposed for the KSI reaction are the catalytic diad and the cooperative hydrogen bond mechanism. Our results from the MD simulations of the enzyme bound substrate and dienolate intermediate strongly support the cooperative hydrogen bond mechanism wherein both Tyr14-OH and Asp99-OD2 are hydrogen bonded to the O3 of steroid. The active site general base, Asp38-CO_2^-, is hydrogen bonded to solvent water only during the MD simulation of E·S. The active site is shielded by hydrophobic residues, which come together and squeeze out the waters from the active site in the E·In complex, thus stabilizing the general acid Asp38-CO_2H.

Abbreviations. KSI, Ketosteroid Isomerase; LBHB, Low-barrier hydrogen bond; *PI, Pseudomonas putida; TI, Pseudomonas testosteroni;* MD, Molecular Dynamics; E·S, Enzyme−Substrate complex; E·In, Enzyme−Intermediate complex; R_X··Y, Distance between atom X and Y.

Acknowledgment. This research was supported by the National Science Foundation Grant No. MCB-9727937. The authors acknowledge National Partnership for Advanced Computational Infrastructure (CRAY T3E at University of Texas Supercomputing Center at Austin), National Computational Science Alliance (SGI Origin 2000 at University of Illinois at Urbana-Champaign) and UC Santa Barbara Supercomputing Facility (SGI Origin 2000) for their generous allocation of computational time. We are grateful to Prof. Ralph M. Pollack for his critical evaluation of the manuscript and helpful suggestions.

Supporting Information Available: Figures S1 (torsional energy profile in 3-butenal when OC−CC dihedral is near 0°// torsional energy profile in 3-butenal when the CC−CC dihedral is near 120°), S2 (negative and positive correlated motions observed during production phase of MD simulation of E·S and E·In), S3 (individual time series of the Tyr14-Val84 and Asp38-Val84 distances). This material is available free of charge via the Internet at http://pubs.acs.org.

JA030138S

(36) Burley, S. K.; Petsko, G. A. *Adv. Prot. Chem.* **1988**, *39*, 125.